NUKLEONIKA 2015;60(3):581–590
doi: 10.1515/nuka-2015-0111

ORIGINAL PAPER

DE GRUYTER
OPEN

Modeling minor actinide multiple recycling in a lead-cooled fast reactor to demonstrate a fuel cycle without long-lived nuclear waste

Przemysław Stanisz, Jerzy Cetnar, Grażyna Domańska

Abstract. The concept of closed nuclear fuel cycle seems to be the most promising options for the efficient usage of the nuclear energy resources. However, it can be implemented only in fast breeder reactors of the IVth generation, which are characterized by the fast neutron spectrum. The lead-cooled fast reactor (LFR) was defined and studied on the level of technical design in order to demonstrate its performance and reliability within the European collaboration on ELSY (European Lead-cooled System) and LEADER (Lead-cooled European Advanced Demonstration Reactor) projects. It has been demonstrated that LFR meets the requirements of the closed nuclear fuel cycle, where plutonium and minor actinides (MA) are recycled for reuse, thereby producing no MA waste. In this study, the most promising option was realized when entire Pu + MA material is fully recycled to produce a new batch of fuel without partitioning. This is the concept of a fuel cycle which asymptotically tends to the adiabatic equilibrium, where the concentrations of plutonium and MA at the beginning of the cycle are restored in the subsequent cycle in the combined process of fuel transmutation and cooling, removal of fission products (FPs), and admixture of depleted uranium. In this way, generation of nuclear waste containing radioactive plutonium and MA can be eliminated. The paper shows methodology applied to the LFR equilibrium fuel cycle assessment, which was developed for the Monte Carlo continuous energy burnup (MCB) code, equipped with enhanced modules for material processing and fuel handling. The numerical analysis of the reactor core concerns multiple recycling and recovery of long-lived nuclides and their influence on safety parameters. The paper also presents a general concept of the novel IVth generation breeder reactor with equilibrium fuel and its future role in the management of MA.

Key words: adiabatic reactor • closed nuclear fuel cycle • lead-cooled fast reactor (LFR) • nuclear reactor core design

P. Stanisz✉, J. Cetnar, G. Domańska
Department of Nuclear Energy,
Faculty of Energy and Fuels,
AGH University of Science and Technology,
30 Mickiewicza Ave., 30-059 Krakow, Poland,
Tel.: +48 12 617 2954, Fax: +48 12 617 4547,
E-mail: pstanisz@agh.edu.pl

Received: 9 October 2014
Accepted: 20 May 2015

Introduction

Within the Generation IV International Forum (GIF) [1], six reactors types were indicated. Three of the six are fast neutron reactors and one can be built as a fast reactor. The main reason why GIF distinguishes fast reactors is the capability of burning minor actinides (MA) and breeding fissile nuclides from ^{238}U [2]. These features of fast reactors can minimize the mass and radioactivity of the long-lived radioactive waste. One of the most likely to be deployed fast reactor technology is the lead-cooled fast reactor (LFR). The European design of an industrially sized LFR facility was prepared at the National Agency for New Technologies, Energy and the Environment (ENEA) in Italy, with the assistance of the AGH University of Science and Technology in Krakow, Poland, within the Sixth Framework Programme ELSY (European Lead-cooled System) project. A few core designs were investigated. With regard to the fuel cycle strategy, only a single-batch option was analyzed. Currently,

the development of the European Lead-cooled Fast Reactor (ELFR) is being continued in the LEADER (Lead-cooled European Advanced Demonstration Reactor) Seventh Framework Programme project based on the achievements of the preceding ELSY project. After the in-depth review of the ELSY design, a new important goal was established at the beginning of the LEADER project – developing the capability of closed fuel cycle.

In the Generation-IV reactor design concepts, there is a possibility of implementing a closed fuel cycle strategy in which all actinides in the spent fuel are reprocessed to form new fuel and recycled in the same reactor. This method retains all actinides inside the reactor with no external mass transport of actinides to or from the environment. Such a situation refers to an adiabatic process, which occurs when there is no transfer between a system and its surroundings. The only exchange is fuel input: natural or depleted uranium (^{nat}U or ^{dep}U), and the fuel output being only the fission products (FPs) and the reprocessing losses. One of the LEADER goals was to prove the feasibility of the adiabatic core by ELFR and to present a cycle-to-cycle method which can lead the fuel vector to equilibrium.

In this paper, the applied methodology, based on the full-core Monte Carlo calculation, is presented. The following sections describe ELFR core and fuel management strategy with the applied method. Results present the reference concept with evaluation that was established by presenting main core characterization at the beginning of life (BOL) and equilibrium state.

Meaning of fuel cycle strategy

The fuel cycle strategy, applicable to a particular nuclear reactor, influences the management of nuclear fuel and radioactive waste. It plays an important role in many aspects of the nuclear system, such as economy, sustainability, security of supply, radiological hazard, public acceptance, political acceptance, and proliferation threats. As some approaches to the fuel cycle strategy may favor one aspect of the cycle, they can fail to produce satisfying outcomes in other aspects. The trade-offs between the different aspects always exist, and it may result in the fuel cycle strategy preferences. In this regard, the fuel breeding is of the highest priorities for the times when the resources of ^{235}U will become scarce. The fuel breeding needs to be the main incentive to undertake the development of Generation IV reactors. The prevailing number of fast breed reactors should be optimized. The major concern results from the production of MA as a result of the nuclear transmutations that accompany the fuel breeding. The fuel cycle strategy in LFR can serve specific needs of its operator, depending on the actual circumstances in the nuclear fuel market or regulatory constraints in relation to the plutonium stockpile or even to the costs of MA management, including its separation or underground storage. The fuel cycle strategy must be properly managed because the increase in radiological hazard can negatively affect the public acceptance of a chosen solution. One of the main objectives of the LEADER projects was the development of a lead-cooled fast neutron reactor with fuel self-sufficiency and improvement in the management of high-level radioactive wastes through the transmutation of MA, by recycling and then burning all the MA mass, so that only FPs would be waste; thereby the period over which high-level radioactive waste remains hazardous could theoretically be reduced.

The reference LEADER core

The reference reactor core proposed as an application of the equilibrium approaches is based on the 1500-MWth (600 MWe) ELSY core design [3]. The ELFR core parameters are presented in Table 1. Several parameters were subject of the core characterization analyses, mainly to identify the core power map that would satisfy flat distribution of the power per fuel assembly (FA). This can be achieved only by using different quantities of fissile material throughout the core. The new concept has been proposed by ENEA and Joint Research Centre (JRC) [4], as an alternative to the fuel enrichment zoning. An increase in the annular void of the fuel pins as a measure input for the fuel distribution over the zones will be referred to as the pin annular void zoning. The pin annular void zoning requires only single fuel enrichment during both irradiation and processing. Optimization of zoning and annular dimensions has been performed. The result illustrated in Fig. 1 shows two regions with different inner hold diameter pellets encapsulated in 169 pins per assembly were proposed. Hundred and fifty seven FAs in the INNER region, where the fuel pellets have a 4-mm diameter hole, and 270 FAs in the OUTER region, where the

Table 1. ELFR main core parameters

Parameters	ELFR
Thermal power [MW]	1500
Number of FAs (INN/INT/OUT) (IN/OUT)	427 (157/270)
Number of pins/FA	169
Active height [cm]	140
Pins pitch [mm]	15.0
FA wrapper outer flat-to-flat [mm]	204.0
FA wrapper thickness [mm]	4.0
FA wrapper inner flat-to-flat [mm]	196.0
FA out-to-out wrappers clearance [mm]	5.0
FA pitch [mm]	209.0
Clad outer diameter [mm]	10.5
Clad thickness [mm]	0.60
Clad inner diameter [mm]	9.3
Gap thickness [mm]	0.15
Pellet outer diameter [mm]	9.0
Pellet hole diameter [mm]	4.0/2.0 (IN/OUT)
Coolant velocity [m/s]	1.53
Number of CRs	12
Number of SRs	12
Number of dummy elements	132

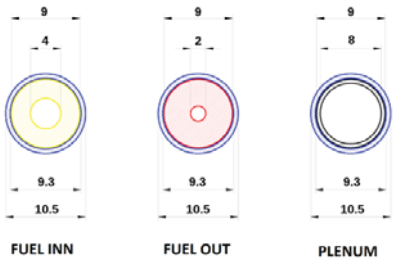

Fig. 1. Fuel pin design for ELFR core configuration in the two zones (all dimensions in millimeter).

Fig. 2. ELFR core configuration with INN (yellow) and OUT (red) FA positions surrounded by dummy elements (white). Blue and green hexagons represent control and shutdown assemblies, respectively.

fuel pellets have a 2-mm diameter hole. Together with the fuel placement, the reactivity control system consists of 12 control rods (CR) and 12 safety rods (SR) distributed evenly through the core in order to avoid pushing the power distribution to the center of the core. The cross-sectional view of the fuel pins in the different zones and the distribution of the FAs between the two zones – together with CRs and SRs positioning throughout the core map – are shown in Fig. 2. The presented FA placement and positions for CRs and SRs satisfy the acceptable power/FA distribution factor, which means that the limits on the maximum temperature of the fuel and the outer surface of the cladding are respected.

Introduction to MCB

The Monte Carlo burnup (MCB) code is a software specifically designed for a detailed burnup calculation based on a three-dimensional transport continuous-energy Monte Carlo n-particle transport code (MCNP) version 5 [5]. In the MCB, the nuclide densities are calculated using the transmutation chains obtained by the transmutation trajectory analysis (TTA) [6] algorithm. The essence of this method is that a variety event system of all possible decay and transmutation reactions can be decomposed into a set of linear chains consisting of all possible routes, or trajectories, through the calculated event. The TTA method is characterized by high accuracy where control of a cut-off parameter is introduced as a precision parameter of calculated trajectory. The concentration of yield nuclides is calculated using the initial composition and constructed transmutation mass flow balance equation.

The MCB code was developed at the KTH, Stockholm. Subsequently, the development has been continued at the AGH until now. After realized version of MCB1C [7] in 2002, the code became available to the scientific community on a freeware basis though the Nuclear Energy Agency Data Bank, Package-ID: NEA-1643. The management program has a lot of computational functions that allow calculating various reactor problems. Recently, new procedures have been added to the MCB code. New procedures make it possible to manage and manipulate fuel outside core, connected with existing features concerning shuffling, mixing, and so on. We can simulate any scenario for utilization of the fuel. By handling core parameters, such as reloading pattern, cooling time, reprocessing losses, feed composition, and mass of actinides in manufacture, we are able to reach any equilibrium state of fuel.

Equilibrium and adiabatic cycle description

The adiabatic core concept is a solution in which the nuclear system that is composed of a fuel factory, reactor park, and the final waste repository, once the waste reaches its equilibrium, needs an external supply of fertile material and turns into waste the FPs only. As LFR is designed for the uranium-plutonium cycle, the fertile material must consist mostly of depleted uranium. The adiabatic cycle characterizes self-breeding cores. However, other heavy metal (HM) nuclides may also be included, that is, actinides fraction from LWR nuclear. It has to be mentioned here that once the cycle has additional fuel contribution in the initial fuel cycle or when there is surplus unloaded fuel, it cannot be considered adiabatic. But because LFR system is flexible in terms of fuel breeding capabilities, it can be designed as a breeder or burner and that system can reach its equilibrium composition. Summarizing, one can distinguish the following fuel cycle strategy applicable to the uranium-plutonium cycle, with the respective equilibrium characterization.

Cycles without external MA loads:

- Adiabatic cycle. The fertile material is only composed of depleted uranium only. All HM nuclides are recycled. Net production of HM nuclides other than fertile is zero. ^{238}U is reduced.
- Breeding cycle. The fertile material comprises depleted uranium only. The fuel is breed, and then it is partially recycled and partially exported to make the initial load of a new system. ^{238}U is reduced.
- Burning cycle. At the front end, a fresh load of plutonium or MOX must be added to the fertile material. The fuel is net burned, which serves to reduce the plutonium stockpile from LWRs.

Cycles with external MA added at the front end to the recycled fuel:

- Adiabatic cycle. At the front end, the fuel is made of the recycled fuel, external MA, and depleted uranium. External MA is burned, all remaining HM nuclides are recycled and ^{238}U is reduced.
- Breeding cycle. At the front end, the fuel is made of the recycled fuel, external MA, and depleted uranium. The fuel is bred but external

MA is burned. The fuel is partially recycled and partially exported to a new system. ^{238}U and MA are reduced.
– Burning cycle. At the front end, the fuel is made of the recycled fuel, depleted uranium, and a fresh load plutonium or MOX with MA. The fuel is net burned including external MA, which serves to reduce the plutonium and MA stockpile from LWRs or fast neutron systems.

The first case (the adiabatic without external MA) is the reference cycle, while the other cases are a departure from it. This departure may be large, following a designer's intention or a small one as a result of differences between the calculation model and reality, or owing to the change in the fuel cycle operational conditions that break design constrains of the adiabatic cycle. Understanding the way and quantitative consequences of the cycle deviation from its adiabatic state may be important for undertaking required countermeasures in the real operation. Investigation of that process has also been carried out. The presented work considers only a reference case for the follow-up study.

In the adiabatic cycle, all HM nuclides are recycled into the new fuel loads after a suitable cooling time, while conserving its total circulating mass. The HM mass deficit at the discharge time is covered by an external amount of fertile nuclide – here depleted uranium is applied because of its wide availability. The state of adiabatic equilibrium cannot be reached quickly, because it is obtained when the production and destruction of every HM nuclide is balanced but the fertile one is established over the applied period of irradiation and cooling. The fertile nuclide undergoes net destruction during that time but then its missing mass is admixed during the new fuel production process at the front end of the cycle. The described process of the nuclide evolutions can also be analyzed in reference to the fuel composition. Once the equilibrium cycle is established, then one can determine quantitatively the equilibrium fuel composition. This, however, has to be given with reference to the time in the period of the entire cycle, because different isotopes over the irradiation and cooling times reach their production-removal balance at different times, depending mostly on the decay rate. In this paper, we mainly use the most extreme cases: beginning of cycle (BOC) and equilibrium reached when no changes in the fuel vector occur.

MCB implementation

The general concept of adiabatic core described earlier can be realized in many ways. In this study for burnup calculations, a detailed pin-by-pin model with 180 burnup zones (10 axial and 18 radial zones) was chosen for demonstration. In order to improve the burnup and relax the initial reactivity constraint, the consideration of a multi-batch core was performed. For establishing a proper amount of batches, we have to consider their influence in many aspects. Larger number of multi-batch will reduce reactivity swing during operation, which is the main advantage. On the other hand, larger amount of FP will remain in the core, resulting in a decrease of the total reactivity, which will have an impact on the cycle length and residence time of fuel and this will force more frequent stops during operation. Finally, to meet the peak pin burnup at the target level of 100 MWd/kg, two-batch map refuelling of the core was adopted with residence time of 5 years. Each batch position is placed with maximum evenness of assemblies and threefold rotational symmetry (Fig. 3). Proposed reference description keeps the limits imposed by material restrictions and maximizes the availability factor of the plant economy. The two-batch reloading scheme takes place without the fuel element shuffling. This means that fuel elements that have served one cycle are not displaced during reloading but merely replaced by fresh ones after the next cycle (this approach also minimizes the probability of making an error during shuffling).

Table 2. Reference two-batch core zone structure with uniform enrichment

Zone	1	2	3
Fuel pin annular void radius [mm]	2	1	1
No. of fuel assemblies	157	96	174
No. of CR assemblies	6	6	12
No. of burnup regions	2 × 3	2 × 2	2 × 3
Fuel assemblies in region	9(10)/30/39	21/27	24/33/30
Pu enrichment [wt%]	18.15		
Fuel irradiation time	2 × 900 days		
Cooling before recycling	7.5 years		

Core design options with a few fuel enrichment zones allow designers to optimize the core and thus to flatten power distribution. A decision was made to abstain from using different plutonium enrichment zones and to perform the radial power shaping only by geometrical means – in this specific case, by varying the central pellet hole diameter (Table 2). One single enrichment zone approach would be sufficient for that purpose and it would simplify reprocessing.

In the two-batch refuelling scheme of a 900-day (approx. 2.5 year) cycles, a 7.5-year cooling time was proposed. The result is that every batch is burnt twice and cooled thrice before reprocessing and reloading it into the core. Five batches make up the system inventory. Two of them are on load, while three are off load (Fig. 4). At the BOL, the fuel consists of depleted uranium and MOX with MA contribution for all fuel assemblies. As the cycle length is affected by breeding gain, we are able to adjust the desired plutonium enrichment to 18.15%. MA composition was characteristic for LWR waste. In the previous studies, the solution of the extended equilibrium state [8] was used to find MA contribution, where mass fraction was established at 1.347%.

One of the main benefits from the directed method performed by MCB is the information about the duration of the multicycle-to-cycle time adjustment and impact from evolution of the spatial distribution. The evolution of the fuel composition

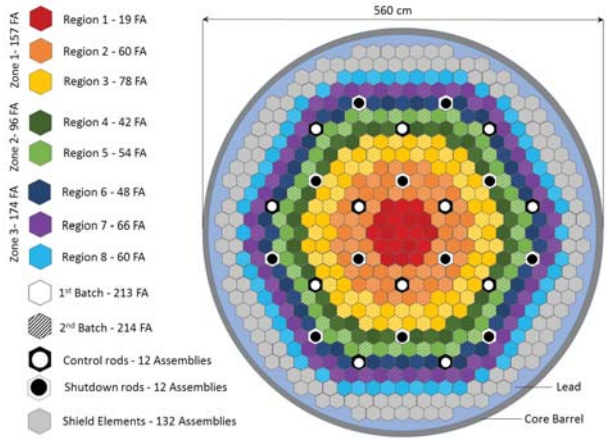

Fig. 3. ELFR core configuration with division of burnup zones. Dashed and colored elements represents adequate burnup zones together with distinction between first and second batch.

is controlled by radioactive decay and reaction rates transmutation. A nuclide can transmute into another one or disappear by fission. The number of created or removed isotopes occurring depends on their abundance in the fuel. Each transmutation reaction removes an isotope and creates a different one. Apart from that, fission reactions remove isotopes from the fuel inventory, while the reloading of the depleted uranium replaces those FPs in equal mass.

Results

Each transport simulation was performed using 30 skipped cycles, 150 active cycles, and 50 000 neutron histories per cycle. JEFF-3.1 [9] based on continuous-energy cross-section libraries with unresolved resonance probability were used by MCB. The libraries incorporate the decay scheme for about 2400 isotopes based on the Table of Isotopes 8E [10].

Initially, in order to establish the equilibrium state, we investigate the changes from cycle-to-cycle in any isotope. Owing to multirecycling, equilibrium state was reached after 600 years. This date is of course symbolic because most nuclide mass density flow transfers to their final concentration much faster. The observed trend shows that isotopes with higher mass and atomic number (such as curium, berkelium, and californium) arise much slower. They also result in some operational problems, which are described in the following section. Nevertheless, the main parameter of core characteristic is reached after approx. 50 years. Comparison between the fuel compositions from fresh load and adiabatic state is shown in Table 3. As BOL vectors differ from the equilibrium ones, we can observe mass flows between elements. An expected final MA and Pu contribution is close to the initial one. We are able to recognize the main transition in the fuel. The ^{238}U is the most dominant isotope and its masses convert to their equilibrium levels the earliest. Its transmutation loss to ^{239}Np on load is compensated in reprocessing. Small amount of ^{235}U decreases during irradiation, which is connected to its fissionability. The ^{239}Pu is the most abundant fissile isotope in the ELFR and its generation or removal rate influences the majority of nuclear parameters. The reduced abundance in adiabatic state is connected to the lower reactivity of the core. Americium is the main MA component, but LWR spent fuel vector contains it in a higher amount than the adiabatic composition; therefore, it is burned. Curium is net produced because its production rate at the operating concentration grows with time. Recognition of these nuclides is important for estimation of nuclides with higher masses such as berkelium and californium, which, because of its small contribution, has not been taken into account in this table.

Criticality evolution

The criticality evolution for a case with CRs fully withdrawn and inserted is presented in Fig. 5. The

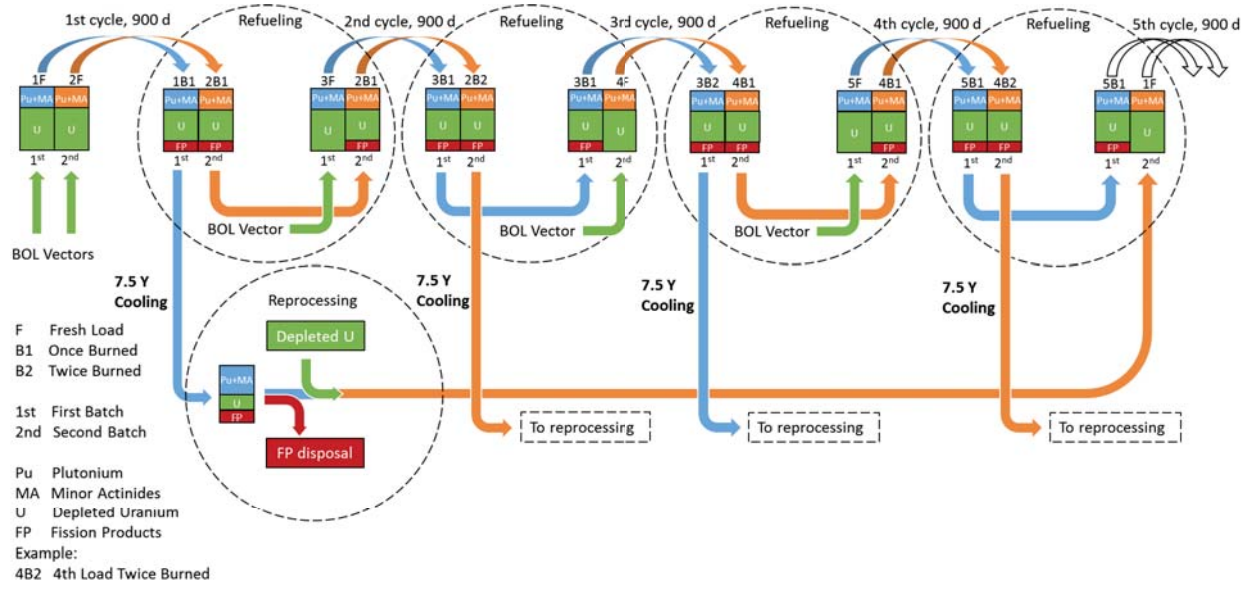

Fig. 4. Flowchart of MCB procedure used to reach adiabatic state.

Table 3. Comparison of fuel vectors and compositions at BOL and in adiabatic equilibrium

Nuclide	Vector fraction in HM [wt%]		Nuclide fraction in HM [wt%]		Nuclide fraction in the vector [wt%]		Element fraction in the vector [wt%]	
	BOL	Adiabatic	BOL	Adiabatic	BOL	Adiabatic	BOL	Adiabatic
				Uranium vector				
^{233}U			–	0.000017	–	0.000021		
^{234}U			0.0020	0.2632	0.0025	0.3265		
^{235}U	80.50	80.59	0.325	0.119	0.400	0.148	100	100
^{236}U			0.008	0.198	0.010	0.245		
^{238}U			80.17	80.01	99.58	99.28		
				Plutonium vector				
^{238}Pu			0.423	0.469	2.330	2.591		
^{239}Pu			10.32	9.979	56.87	55.19		
^{240}Pu	18.15	18.08	4.90	6.54	27.00	36.19	100	100
^{241}Pu			1.108	0.455	6.100	2.517		
^{242}Pu			1.396	0.634	7.69	3.51		
^{244}Pu			–	0.00028	–	0.00152		
				MA vector (Np + Am + Cm)				
^{237}Np			0.05	0.120	3.81	8.98	3.81	8.98
^{241}Am			1.016	0.817	75.41	61.31		
^{242m}Am			0.003	0.061	0.25	4.60	91.84	80.68
^{243}Am			0.218	0.197	16.17	14.77		
^{242}Cm			–	0.0001	–	0.011		
^{243}Cm	1.347	1.332	0.0009	0.0021	0.067	0.158		
^{244}Cm			0.041	0.082	3.04	6.17		
^{245}Cm			0.016	0.027	1.16	2.05	4.35	10.34
^{246}Cm			0.0012	0.0189	0.090	1.42		
^{247}Cm			0.000023	0.0037	0.0017	0.279		
^{248}Cm			0.000002	0.0034	0.0001	0.256		

reactivity swing, which occurs from BOL to the time of reactivity stabilizations, spans almost the entire range of the CR system reactivity margin. The reactivity is highest at BOL and drops with every cycle until the equilibrium level is reached. The initial reactivity in the reference core can be fully managed by the designed CR bank, which at BOL reactivity margin equals 5.293(±25) pcm. The CR insertion may mainly affect reduction of the plutonium fraction. The effect of CR insertion on the reactivity and the magnitude of this effect needs to be understood in order to become aware of how much a deeper CR insertion during a cycle can shorten the cycle length. A deeper insertion might be the consequence of differences between theory and reality or a deviation from the assumed fuel strategy. CR insertion increases the cycle reactivity swings – negative on load and positive off load. The insertion increases the negative reactivity over entire cycles, where the additional negative swing would reach the level of 1300 pcm with CRs fully inserted comparing BOL with equilibrium. As, in reality, the CRs are partially inserted only in the initial cycles, the CRs insertion will have the greatest impact at the beginning and additional swing will be reduced during the approach of the equilibrium.

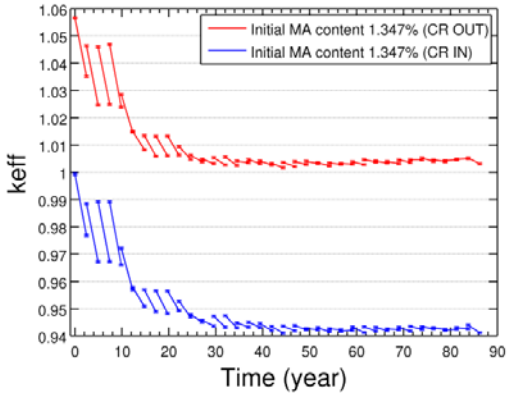

Fig. 5. Effect of control rods insertion on criticality (k_{eff}) evolution of the LFR core case.

Core characteristics

The assessment of the LFR core was characterized by fuel power densities and linear power ratings used for thermal hydraulics. The assessment is presented at BOC and EOC of the first cycle and at the equilibrium point. The distributions of fuel power densities that are applicable for burnup calculations are given together with linear power ratings that are applicable to thermal-hydraulic assessment. Distributions of those functions are usually the same, but in our case, the fuel pellet does not have a uniform cross section, and therefore, that distribution differs and can serve as an initial parameter. Presented cases consider in turn CRs withdrawn and fully inserted in order to assess their influence on the changes in power distribution resulting from partial insertion of CR.

In Fig. 6, the power distribution is obtained at the fresh start where the contribution of FPs initially is zero. Together with equilibrium case in Fig. 7, the results represent two most extreme cases. Fuel pow-

er density is higher at BOL where the highest peak density is 480 W/cm³ for the case in which CRs are withdrawn. At EOC of first cycle, the peak density is about 7% smaller than that at BOC. This is due to the lack of FP. On the other hand, in the equilibrium case, the power peak at BOC (444.5 W/cm³) is about 1% smaller than that at BOL, which means a very steady power distribution. The obtained results will not require complicated operations in the flow control. Choosing the appropriate void annular radius in pellets affects linear power rating. Thereby, results depicted in Figs. 8 and 9 are much more appropriate for thermal-hydraulic assessments. The

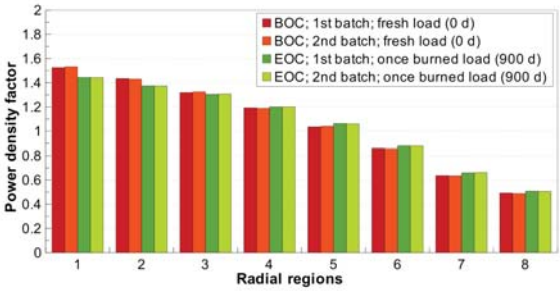

Fig. 6. Radial density power factor at the beginning and end of the first cycle; CR withdrawn.

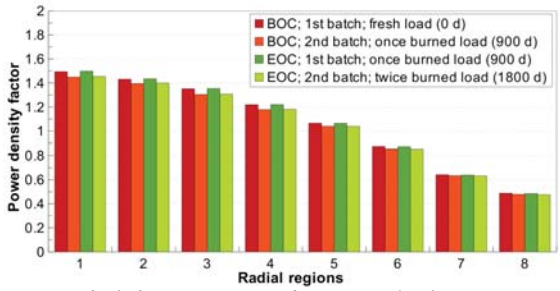

Fig. 7. Radial density power factor at the beginning and end of the adiabatic state; CR withdrawn.

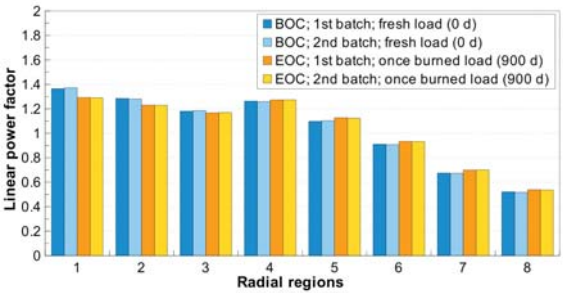

Fig. 8. Linear power factor at the beginning and end of the first cycle; CR withdrawn.

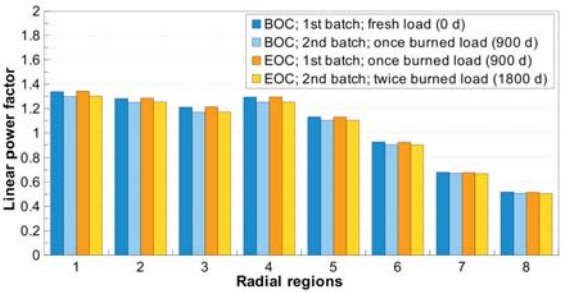

Fig. 9. Linear power factor at the beginning and end of the adiabatic state; CR withdrawn.

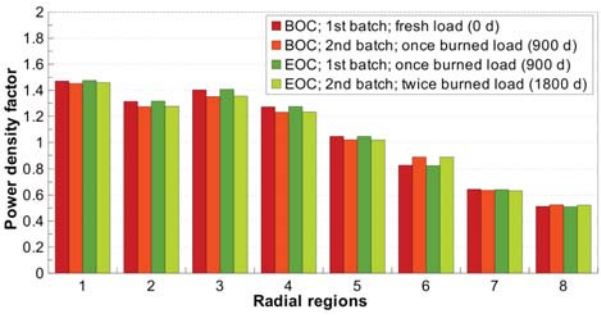

Fig. 10. Radial density power factor at the beginning and end of the adiabatic state; CR fully inserted.

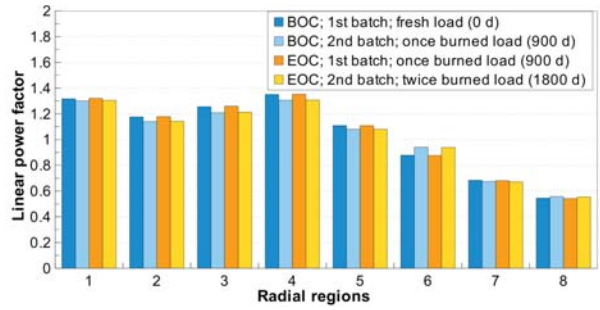

Fig. 11. Linear power factor at the beginning and end of the adiabatic state; CR fully inserted.

case of examination depicted in Figs. 10 and 11 of CR confirms a well-selected distribution in which power pushing is not observed. This may be affected by a partial insertion of the CR during operation. It is an important control issue of the reactor to have stable operation at all times.

Average burnup

The design assumes the burnup limit at 100 MWd/kg. To retain that limit while maintaining a long cycle, large disparities in power distribution have to be avoided. Burnup is generally bound to the constrained thermal power of the system and the cycle period time; therefore, the average burnup discharge values of the fuel should not fluctuate substantially. Some fluctuations in terms of specific energy deposition can occur due to a possible change in the heating fraction outside the fuel. Some of the fluctuations can also be attributed to batch-to-batch fluctuations because the number of core fuel assemblies is an odd number, thus a slightly different amount of HM is loaded every time. FIMA (fusion per initial metal atom) can also float slightly, because the fuel vector transmutation changes the HM vector, which affects to some extent the fission heating number. As shown in the Table 4, an average discharge FIMA decreases slightly with the number of fuel reprocessing from starter first cycle to adiabatic. The other case, with CR inserted, shows the same tendency. The FIMA peak value in all cases is similar, with about 9.83% maximum for adiabatic CR in case where differences between the rest of the cases is rather in the range of statistical fluctuation. The peak burnup is kept within a safe margin to ensure that the average value located in a given volume is lower than the real one, which could

Table 4. Burnup distribution and first fuel cycle and adiabatic state

	Average burnup on discharge [(MWd)/kg]		Average FIMA [%]	
	CR out	CR in	CR out	CR in
First cycle	49.9	48.4	5.51	5.58
Adiabatic	50.2	48.6	5.50	5.56
	Peak values			
First cycle	87.9	85.8	9.72	9.48
Adiabatic	88.3	86.1	9.67	9.83

be higher in certain point. Thus the higher calculated burnup is located in the first region for adiabatic case (CR withdrawn) and equals 88.3 MWd/kg while the average is 50.2 MWd/kg.

Safety-related coefficients

Safety-related coefficients were calculated for the first cycle and adiabatic cycle from BOL and EOC, respectively. They are shown in Table 5. They were obtained with all CRs withdrawn. The Doppler constants are negative between 722 and 825 pcm, while the core expansion coefficients are negative from 242 to 345 pcm for 2% axial expansion and from 822 to 909 pcm for 2% radial expansion. The void worth is generally negative for entire vessel voiding but active core voiding is rather strongly positive. Safety-related parameters do not change significantly with a different MA content or fractions at BOL. Also voiding the vessel to the bottom fuel level brings positive void reactivity between 1299 and 1915 pcm. It was noticed that a very strong effect on void coefficients is brought by CR insertion level. In the applied model, all CR are in the most remote positions from the core centre. The insertion of the CRs can shift down the void worth more than 1500 pcm (independently from bringing the reactivity down); therefore, with the CR inserted, the vessel voiding should decrease the reactivity. Generally, an increased MA content increases positive terms in reactivity coefficients; therefore, it will need attention and possibly a consideration of additional reactivity countermeasures at the reactor peripheries.

Fuel handling issues

Approaching an equilibrium connected with the multirecycling closed cycle creates some hazards

Table 5. Safety-related coefficients in the first fuel cycle and adiabatic state

Source of change		First cycle		Adiabatic	
		BOL	EOC	BOL	EOC
		Reactivity change [pcm]			
Dopler constant		–825 ± 70	−730 ± 38	–785 ± 23	−722 ± 25
Core 2% axial expansion		–242 ± 23	−277 ± 23	–265 ± 25	−345 ± 23
Core 2% radial expansion		–823 ± 23	−822 ± 23	–909 ± 25	−891 ± 25
Cladding 2% expansion		93 ± 24	40 ± 23	112 ± 25	124 ± 23
200 K coolant temperature change		91 ± 22	77 ± 23	117 ± 25	33 ± 25
Void worths:					
– active core coolant	–10%	463 ± 25	439 ± 23	503 ± 23	476 ± 25
– density change:	–20%	844 ± 25	841 ± 23	923 ± 23	931 ± 25
	–30%	1270 ± 25	1296 ± 22	1441 ± 25	1372 ± 25
Active core voiding (100%)		3897 ± 25	4093 ± 23	4589 ± 25	4469 ± 24
Entire vessel voiding (100%)		–1549 ± 25	–1383 ± 26	–1001 ± 24	–1095 ± 24
Reactor vessel voiding to the level	Top	–1075 ± 24	–1135 ± 23	–1110 ± 25	–1149 ± 25
of duel elements:	Bottom	1299 ± 25	1524 ± 23	1915 ± 25	1778 ± 26
Control rod worths (12 CR)		–5293 ± 25	–5327 ± 23	–5466 ± 28	–5533 ± 24

Table 6. Neutron emission and principle contributors [neutrons/(s·kgHM)]

Cooling time [year]	0	2.5	5	7.5
^{239}Pu	1.65×10^{0}	1.74×10^{0}	1.74×10^{0}	1.74×10^{0}
^{240}Pu	6.71×10^{4}	7.12×10^{4}	7.13×10^{4}	7.13×10^{4}
^{235}U	1.02×10^{-5}	1.09×10^{-5}	1.10×10^{-5}	1.11×10^{-5}
^{238}U	1.01×10^{1}	1.07×10^{1}	1.07×10^{1}	1.07×10^{1}
^{242}Cm	4.09×10^{6}	1.19×10^{5}	3.19×10^{4}	2.98×10^{4}
^{244}Cm	1.22×10^{7}	1.18×10^{7}	1.07×10^{7}	9.73×10^{6}
^{246}Cm	1.66×10^{6}	1.76×10^{6}	1.76×10^{6}	1.76×10^{6}
^{248}Cm	1.42×10^{6}	1.50×10^{6}	1.50×10^{6}	1.50×10^{6}
^{250}Cm	1.13×10^{3}	1.19×10^{3}	1.19×10^{3}	1.19×10^{3}
^{249}Bk	5.11×10^{1}	7.48×10^{0}	1.04×10^{0}	1.43×10^{-1}
^{250}Cf	7.84×10^{6}	7.27×10^{6}	6.37×10^{6}	5.58×10^{6}
^{252}Cf	1.39×10^{7}	7.66×10^{6}	3.97×10^{6}	2.06×10^{6}
^{249}Cf	8.11×10^{0}	9.82×10^{0}	9.95×10^{0}	9.93×10^{0}

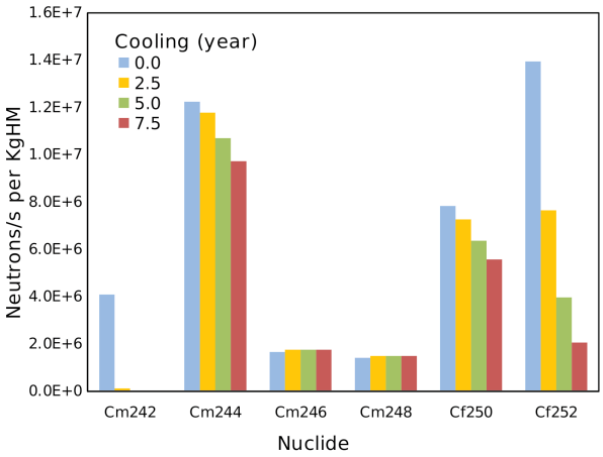

Fig. 12. Neutron emission from main contributed actinides.

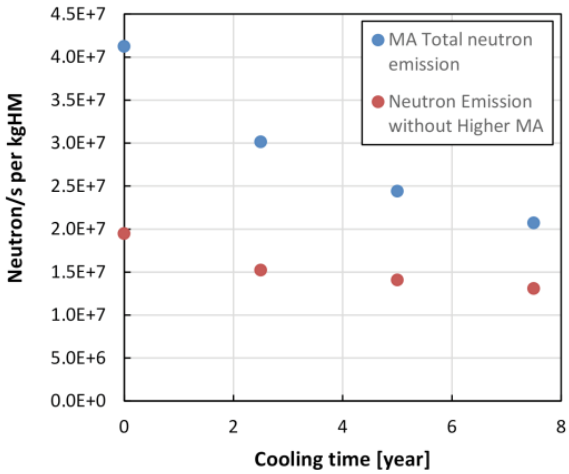

Fig. 13. Neutron emission with and without Cf and Bk.

on the part of the recycled fuel. Keeping MA in the reactor fuel cycle as a repository environment can cause some handling complications with reprocessing spent fuel. Higher actinides (HA) such as berkelium and californium buildup during operation with multirecycling. The occurrences of those isotopes are irrelevant to neutron and cycle properties during operation. However, some of their isotopes are strong neutron emitters from spontaneous fission. In general, the separation process poses difficulties, creating a negative impact throughout increased temperature and ionizing radiation. Additional radiation from neutron sources may hinder the process. The protection of workers at the separation and fabrication plants would be complicated by the relatively high neutron emission rates of the MA.

Table 6 and Fig. 12 compare the neutron emission of the HM discharged load at the EOC after reaching equilibrium as a function of cooling time. The table presents the major contribution of isotopes to the total neutron emission as well as the total neutron emission generated by the actinides in the fuel. An increase of about 110% at discharge before cooling and 60% after cooling is observed when counting the higher MA as californium (Fig. 13). This increase is attributed mainly to the presence of ^{250}Cf and ^{252}Cf, which are neglected in most models.

The neutron emission rate was generally lower in the first few fuel recycle stages than when isotopes have passed the saturation point where their concentration can vary. Therefore, neutron emission should be analyzed at each state of reaching equilibrium. To understand the impact of a higher MA on fuel during multirecycling better, nuclear data needs to be prepared. The problem of estimating a neutron source with higher concentration of actinide arises because impact from all previous isotopes concentration and cross sections together with uncertainty will affect the buildup process. An increase or a decrease in the neutron emission estimation will be possible with a more accurate measurement of crucial cross sections present in significant reactions.

Conclusions

Multirecycling of MA is the most beneficial from the repository management point of view. The amount of actinides to be sent to the repository can be significantly reduced by keeping the MA in a fuel cycle. The obtained results were used to set up a reference core configuration of the LEADER project after a thorough review of the ELSY design. A new technical solution has been implemented in the MCB code to reach fuel vector equilibrium in the adiabatic configuration of the core and evaluate the safety response of the system, which helps estimate the advantages of the technology. The reference core has been established using the adiabatic core approach with a feed of natural or depleted uranium. The zero net production of MA has been achieved and adopted for cycle-to-cycle ELFR. This enables production of energy with a minimum release of nuclear waste to the environment – only FPs and reprocessing losses remains. A system designed in that way meets GIF expectations of burning MA and breeding fissile nuclides from ^{238}U. Moreover, this will enable us to extend the present uranium supplies at a rate of at least 100 and eliminate long-term radiotoxicity sources.

Acknowledgments. This work is partially funded by the European Commission under the Seventh EURATOM Framework Program, within the Collaborative Project LEADER *Lead-cooled European Advanced Demonstration Reactor*. In addition, the authors would like to acknowledge the help of the Academic Computer Centre CYFRONET AGH where the design and development of the aforementioned tools is being carried out.

References

1. GIF. (2002). *A Technology Roadmap for Generation IV Nuclear Energy Systems*. U.S. DOE and the Generation IV International Forum.
2. GIF. (2006). *The U.S. Generation IV Fast Reactors Strategy*. U.S. DOE. (DOE/NE-0130).
3. Cinotti, L., Smith, C. F., Siennicki, J. J., & *et al.* (2007). *The potential of the LFR and the ELSY project*. Nice, France: ICAPP'07.

4. Döderlein, C., Cetnar, J., Grasso, G., & *et al*. (2013). *Definition of the ELFR core and neutronic characterization*. (Technical Report LEADER-DEL 005-2011, WP2, LEADER Project).
5. X-5 Monte Carlo Team. (2003). *MCNP – A General Monte Carlo N-Particle Transport Code, Version 5*. Los Alamos: Los Alamos National Laboratory. (LA-UR-03-1987).
6. Cetnar, J. (2006). General solution of Bateman equations for nuclear transmutations. *Ann. Nucl. Energy*, *33*(7), 640–645.
7. Cetnar, J., Gudowski, W., & Wallenius, J. (1999). *MCB: A Continuous Energy Monte Carlo Burnup Simulation Code. Actinide and Fission Product Partitioning and Transmutation*. (EUR 18898 EN, OECD/NEA 523).
8. Artioli, C., Grasso, G., & Petrovich, C. (2010). A new paradigm for core design aimed at the sustainability of nuclear energy: The solution of the extended equilibrium state. *Ann. Nucl. Energy*, *37*, 915–922.
9. NEA/NSC/DOC18. (2006). *Processing of the JEFF-3.1 Cross Section Library into Continuous Energy Monte Carlo Radiation Transport and Criticality Data Library*. http://www.nea.fr/abs/html/nea-1768.html.
10. Firestone, R. B., Shirley, V., Baglin, C., Chu, S., & Zipkin, J. (1996). *Table of Isotopes 8E*. New York: John Wiley & Sons, Inc.